Chapter 3
Estimation of Energy Barrier
in micelle-mediated nucleation growth

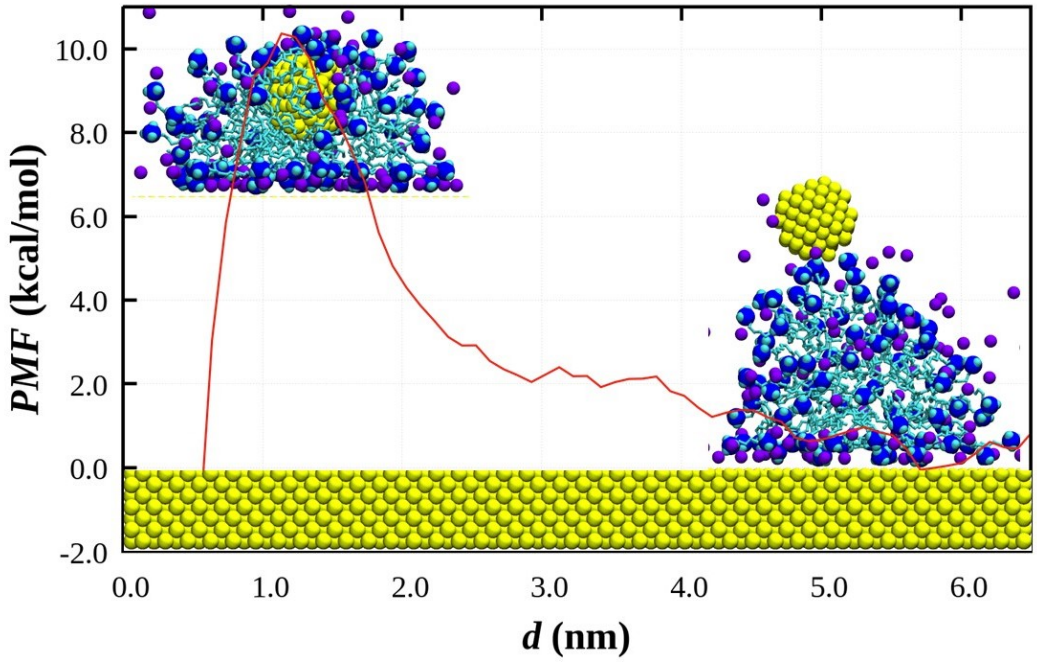

3.1 Introduction

Nanoparticles and their assemblies have revolutionized applications across all engineering, e.g., optics,[114] electronics,[114–119] sensors,[120–122] drug delivery,[123–125] catalysis, [4, 126, 127] bio-imaging,[128] cancer treatment,[129–132] etc. In all these applications, nanoparticles of different sizes and shapes are often used. In the synthesis of gold nanocrystals of different shapes and sizes, surfactants play a pivotal role in preventing undesirable growth and maintaining the size uniformity during synthesis. Surfactants can adsorb onto the surface of growing nanocrystals, modifying atom attachment's surface energy and kinetics. They can direct the growth process by selectively binding to specific crystal facets, thereby controlling the shape, size and stability of the nanocrystals.

Surfactants also play a key role by acting as capping agents, providing a protective layer around growing nanocrystals and influencing the kinetics of the nucleation and growth. Surfactants influence the nucleation stage by lowering the surface energy and stabilizing small clusters of atoms. This reduction in surface energy can significantly lower the nucleation barrier, facilitating the formation of nanocrystal seeds.[133] Several authors have investigated that the CTAB surfactant can form different mesoscopic aggregates such as micelles[134], rod-like[135] vesicles[136], bilayers[137], and meso-phases with various geometries.[138] It has many applications such as - in DNA extraction because it possesses antibacterial properties,[139] widely used in the synthesis of metallic nanoparticles as a stabilizer and growth driving agent of nanoparticles.[133, 140–143] In aqueous solution, CTAB molecules get ionized into CTA^+ ions and bromide ions. The CTA^+ ions form the micelles, and the counter ions, i.e. bromides, tend to stay near the cationic micellar surface. Many processes are developed to synthesize nanoparticles of different sizes and shapes. However, nanoparticles with appropriate shapes and sizes require understanding the nucleation process in solution. Several authors conducted experiments to understand the nucleation and growth of nanoparticles and developed theories such as LaMer-Brust nucleation mechanisms[44], Oswald ripening[45], Finke-Watzky two-step nucleation mechanism[46], coalescence and orientation attachment mechanism [47, 51] and so forth, which we have discussed in detail in Chapter 1. The metal nanocrystals gradually start nucleation in all of the mechanisms mentioned above, and then autocatalytic development follows. The development of nanoparticles is contingent upon the migration of atoms from the solution to the surface of the nanocrystal. Fick's first law may elucidate the flow of atoms. The atom concentration at a distance from the surface is a crucial regulating parameter.[144] Meena et al.[145] investigated that the interstitial spaces between adjacent micelles form channels that facilitate the direct access and diffusion of ions from the bulk solution to the surface, enabling crystal growth. Their findings indicated that ion diffusion is more efficient toward the (111) facet, leading to the preferential growth of gold nanorods along this direction. Similarly, Silva et al.[146] investigated the role of surface curvature in the growth mechanism of gold nanorods and revealed that

the curvature at the nanorod tips plays a critical role in facilitating ion diffusion. Their study demonstrated that the intermicellar channels formed on curved surfaces are larger and more dynamic compared to flat surfaces, allowing for easier migration of $[AuBr_2]^-$ ions to the surface. This preferential diffusion toward curved regions promotes anisotropic growth at the tips, highlighting the importance of curvature over crystallographic facets in determining the growth direction of gold nanorods. Here, we use molecular dynamics simulations to understand the nucleation of gold atoms and their growth on a gold surface (flat surface or large nanoparticles) mediated by the micelles in solution. We are keen on exploring the role of the micelles in providing a possible path for gold atoms to nucleate onto the surface. Estimation of the free energy barrier for the nucleate to reach the surface can help us in determining the rate of transport to the surface. To answer these questions, randomly distributed gold atoms in the solution lead to the formation of nucleates of different sizes and shapes inside the micelle. Observing the shape, size, and growth of nucleates inside micelles and quantifying the nucleation process through the potential of mean force (PMF) is challenging.

In this study, we are reporting the nucleation of gold nucleates on a gold surface under the influence of CTAB micelles. This study aims to understand the growth of nanocrystals on the gold surface with the presence of CTAB micelle. The micelle acted as a template for the nucleation of seed gold/gold nucleate on the gold surface. The surfactant molecules within the micelle can adsorb onto the gold surface, providing a stable environment for the depositing of gold atoms/gold nucleate. This organized arrangement of surfactant molecules can promote the nucleation of gold atoms/nucleates with controlled size and distribution. Here, we use MD simulations to understand the organized arrangement of CTAB micelles on the gold surface and calculate the free energy barrier associated with the process.

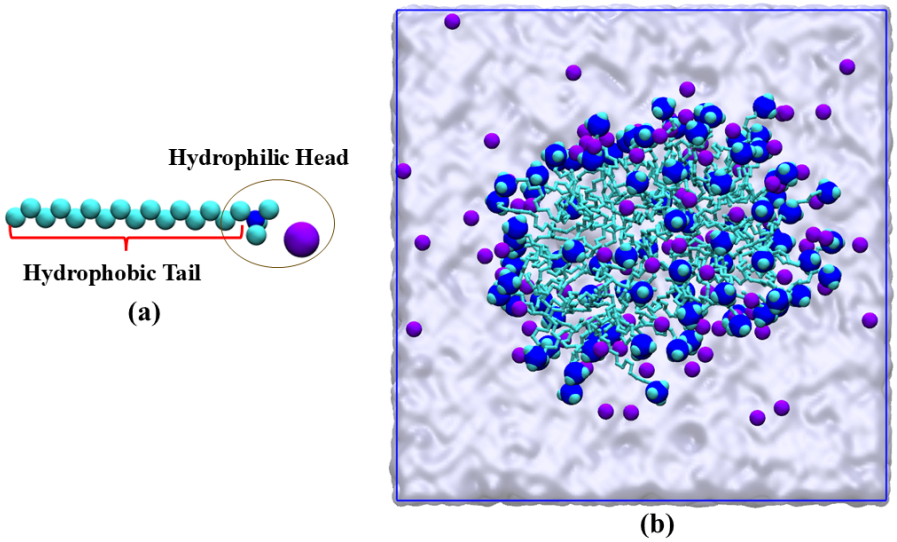

Figure 3.1: (a) CTAB molecule, the nitrogen atom and bromide ion are represented as blue and purple spheres, respectively, and all the methyl groups are represented as cyan spheres. (b) Snapshot of the system containing a micelle of CTAB molecules in an aqueous media. Water has shown an ice-blue colour in continuous media. The blue rectangle represents the periodic box.

3.2 Methodology

A micelle consisting of 90 CTAB molecules was solvated in a simulation box of 4 nm $\times$4 nm $\times$4 nm containing 12000 water molecules. We used Packmol [147] to generate initial configurations. As shown in Figure 3.1(a), a molecular representation of the CTAB molecule, the headgroup of each CTAB molecule comprises trimethylammonium bromide and a hydrocarbon tail. All the CH_3 and CH_2 groups were modelled as united atoms, whereas the head group was modelled explicitly. The charge on the CTA cation was such that the three methyl groups in the headgroup carried a partial positive charge of 0.1701e, the methyl group adjacent to nitrogen carried a partial positive charge of 0.2167e, and the methyl groups in the tail group were set to be neutral. The central nitrogen atom was set to be 0.273e, and the bromide ions carry a charge of -1. All the CH_3 and CH_2 groups were modelled as united atoms, and their interaction parameters are as per GROMOS96-53a6 forcefield.[93] All the non-water molecules were kept fully flexible. The nonbonded interactions between like and alike particles were modelled as per Lennard-Jones 12-6 (LJ-

12-6). The bond stretching and bending were described using harmonic potentials. For nonbonded interactions, a cutoff distance of 12 Å was used. An extended Simple Point Charge (SPC/E) water model was used to model the solvent. All the interaction parameters used in this study are listed in Table 3.1.

The initial configurations of the systems were subjected to energy minimization for 5,000 steps using the steepest descent method. The solutions were equilibrated in an NPT ensemble for 5 nanoseconds. We ran molecular dynamics production runs in an NVT ensemble for 65 nanoseconds, with a timestep of 2 femtoseconds, to use the Velocity Verlet algorithm[148] to integrate the equation of motion. The trajectory was stored at every 1 picosecond. The Parrinello-Rahman barostat (relaxation time is 1.0 picosecond) and the Nosé-Hoover thermostat (relaxation time is 0.5 picosecond) kept the pressure and temperature stable, respectively. All MD simulations were performed using the LAMMPS package.[149] VMD[150] was used to visualize the simulation trajectories. The simulation box was considered periodic in all three directions.

Figure 3.1(b) contains a snapshot of the system after the 5 ns production run we have considered. Different numbers of gold atoms have been dispersed in the solution to mimic the nucleation process of gold atoms in the solution. We have employed Steered Molecular Dynamics (SMD),[151, 152] to calculate the potential of mean force to understand the energy landscape for atoms towards the gold surface. For SMD, different sets (by changing the position of the gold atom/gold nucleate) of configurations are considered to calculate the average potential of mean force.[153] Randomly distributed gold atoms in the solution were allowed to form nucleates of different sizes and shapes. Additional seeds, gold nucleates ($r \sim 1$ nm), were introduced to the system away from the surface to understand the behaviour of seeds. Using the umbrella sampling technique followed by the Weighted Histogram Analysis Method (WHAM),[154] the energy landscape for the fusion of nucleate with the gold surface was calculated.[155]

In the umbrella sampling, a set of evenly spaced 70 windows along the reaction coordinate are subjected to an external biasing potential to accomplish extensive sampling in these

Table 3.1: Force Field Parameters for the CTAB and Water molecules.

Nonbonded Interactions				
Atom	σ_{ij} **(Å)**	ϵ_{ij} **(kcal/mol)**	q **(e)**	
CH_3	3.714	0.1757	0.0	
CH_2	3.733	0.0774	0.0	
CH_2[N]	3.762	0.1232	0.2167	
N	3.087	0.1445	0.273	
CH_3[N]	3.762	0.1232	0.1701	
Br	4.54	0.3972	-1.0	
O	3.166	0.1553	-0.8476	
H	0.0	0.0	0.4238	
Au	2.946	5.306	0.0	
Bond-stretching				
Bond	r_0 **(Å)**	k_b **[kcal/mol.Å^2]**		
N-CH_3	1.47	400		
CH_2-CH_3	1.54	340		
O-H	0.95	500		
Bending				
Angle	θ_0 **(Å)**	k_θ **[kcal/mol.Å^2]**		
N-CH_2-CH_2	109.5	100		
CH_2-CH_2-CH_2	111.4	126.67		
CH_2-N-CH_3	117	151.76		
H-O-H	109.47	500		
Torsion(kcal/mol)				
Dihedral	k_1	k_2	k_3	k_4
N-CH_2-CH_2-CH_3	0.8698	0.9552	0.2979	-0.2283
CH_3-N-CH_2-CH_2	2.9114	-4.3453	2.7226	-1.7675
CH_2-CH_2-CH_2-CH_3	0.0	0.7056	-0.1355	1.5727

windows using a harmonic potential. To eliminate the biasing potential and reconstruct the potential of mean force (PMF), we applied the Weighted Histogram Analysis Method (WHAM).[154] The distance between the centre of mass of the gold nucleate and the upper surface of the gold (111) surface was the reaction coordinate. We performed a 1.0 ns production run in an NVT ensemble for each window at 303.15 K without restraints using a harmonic force constant of 100 kcal/mol.Å^2. In WHAM, the number of bins was set to 100, with a tolerance for iterations was 10^{-5}. We have monitored the size and shape of the micelle by calculating the components of the radius of gyration (R_g) tensor, $R_{g_{xx}}$, $R_{g_{yy}}$, $R_{g_{zz}}$, respectively. We also calculated the order parameter to understand the orientation of

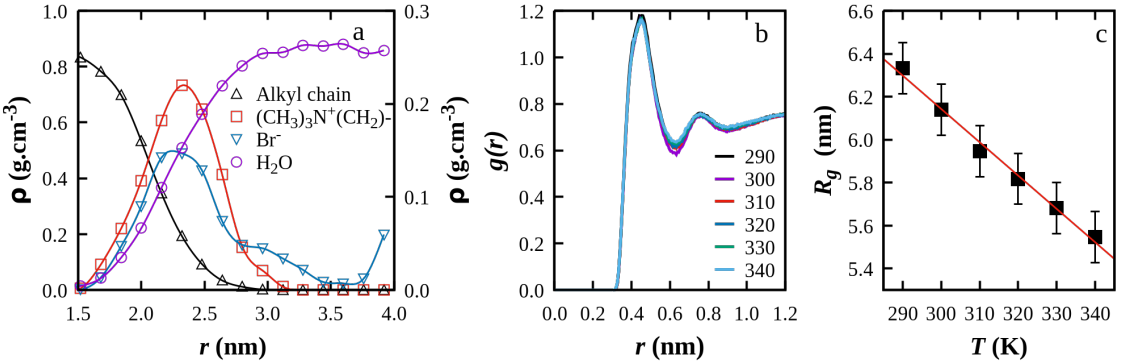

Figure 3.2: (a) Mass density profiles of different segments as a function of distance from the centre of mass of a CTAB micelle at 303 K (b) Radial distribution functions between the oxygen of water and N of the head group at different temperatures (c) Variation of Radius of gyration of the cationic part of micelle with temperature.

the micelle on the gold surface. The order parameter of the micelle molecules is a measure of the degree of ordering and alignment of CTAB molecules within a micelle structure.

3.3 Results and Discussion

We started the discussion with the structure of the CTAB micelle in the solution. Here, we have calculated the structural properties of CTAB micelle in the solution, such as the density profile at 303 K, the radial distribution function, and the radius of gyration at different temperatures. Each of these properties provides insight into different aspects of micelle structure and behaviour in solution. In particular, we calculate mass densities of different components to understand the interaction of CTAB micelle with gold surfaces, along with the order parameter and radius of gyration to understand the orientation and shape of the micelle on gold surfaces. In this study, the structure and properties of the CTAB micelle are critical to its function, making their quantification essential. We begin by analyzing the micelle's organization. CTAB molecules have polar head groups with a positively charged quaternary ammonium ion and a negatively charged bromide ion. In micellar form, the hydrocarbon tails of CTAB molecules are sequestered within a hydrophobic core, shielded from water, while the polar heads orient outward, interacting with and remaining hydrated by the surrounding water molecules, presenting structural properties of the CTAB micelle. In Figure 3.2(a), density profiles for different micelle components—alkyl chains, ammo-

nium groups, bromide ions, and water—illustrate their spatial arrangement. The density profile of the alkyl chains declines gradually from approximately 1.5 nm to zero at about 2.8 nm, indicating that these hydrophobic chains form the micelle core. The ammonium group density profile shows a peak at around 2.25 nm, signifying the micelle's overall size, consistent with literature values.[75] The static profile of ammonium ions suggests that the micelle maintains a spherical structure. The density of water increases to bulk levels from about 1.5 nm outward, highlighting the scarcity of water within the micelle core.

Figure 3.2(b) shows the arrangement of water molecules relative to the nitrogen atom of the head group across different temperatures. At a distance of 6.37 Å from nitrogen, the water molecules form a solvation layer around the head group of each surfactant molecule.[76] Due to heterogeneity in the micelle, the local density of the water did not reach that of the bulk. A larger cut-off distance for the RDF calculation would serve it.

Figure 3.2(c) depicts that the radius of gyration of the micelle's cationic portion decreases with increasing temperature. Higher kinetic energy at elevated temperatures enhances anion mobility, weakening the solvation shell, as reflected in a reduced coordination number. By correlating the ammonium ion's peak density distance from the micelle's centre of mass with the ammonium ion's first hydration cell length, we find a consistent ratio of 2.028 across the temperature range. Additionally, the CTAB micelle's order parameter in bulk solution is 0.30 ± 0.004, remaining stable within the temperature range studied.

Figure 3.3 contains a snapshot of the system we have considered. A solvated micelle of CTAB was allowed to evolve in the presence of a gold surface. We equilibrated micelles on the gold surface to see their interaction with the surface. Introducing a gold surface with a (111) plane creates heterogeneity in the system and adds a vapour-liquid interface of water in the opposite direction. The CTAB micelle becomes strongly adsorbed onto this surface.

Figure 3.4(a) shows the density profiles of various micelle components, indicating a strong inclination toward the surface. Notably, the two sharp peaks in the density profile of water

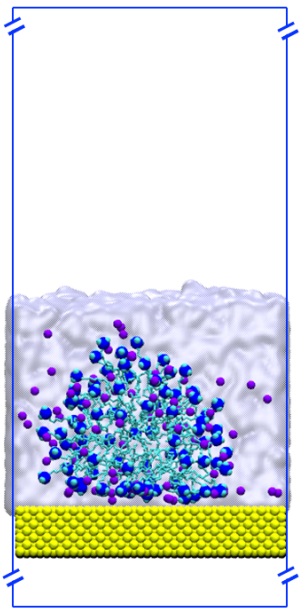

Figure 3.3: Snapshot of the system to show the attachment of CTAB micelles on a gold surface. The Au(111) surface, at the bottom, is represented in yellow spheres. Water molecules have shown an ice-blue colour. The blue rectangle represents the periodic box (not to scale in z-direction)

(purple line) near the surface (with the top of the surface at zero) revealed the formation of a high-density water layer adjacent to the gold surface. The water density increases sharply at a short distance from the surface, forming a high-density layer that extends away from the surface and gradually transitions to bulk density. The density profile of the ammonium group exhibits a sharp peak at ~ 0.42 nm, suggesting strong interactions between the micelle and the first layer of water on the surface. This profile further indicates that the micelle has an overall height of ~ 4.4 nm. Meanwhile, the density profile of the tail methyl group shows a peak around 0.6 nm from the surface, suggesting a layered arrangement within the micelle. The strong adsorption of ammonium ions at the surface results in the ordered structuring of the alkyl chains near the gold surface. The order parameter (S_{zz}) of the CTAB micelle on the gold surface is 0.405 ± 0.008, which is higher than in the bulk phase. This increase suggests that some micelle molecules are reorganizing into a bilayer-like structure. The water layer at the gold surface in the presence of the micelle exhibits a strong correlation, as shown by the 2D radial distribution function (RDF) of water on the surface in Figure 3.4(b), with a prominent peak in the density profile supporting this finding. Additionally, the ammonium and bromide ions display a

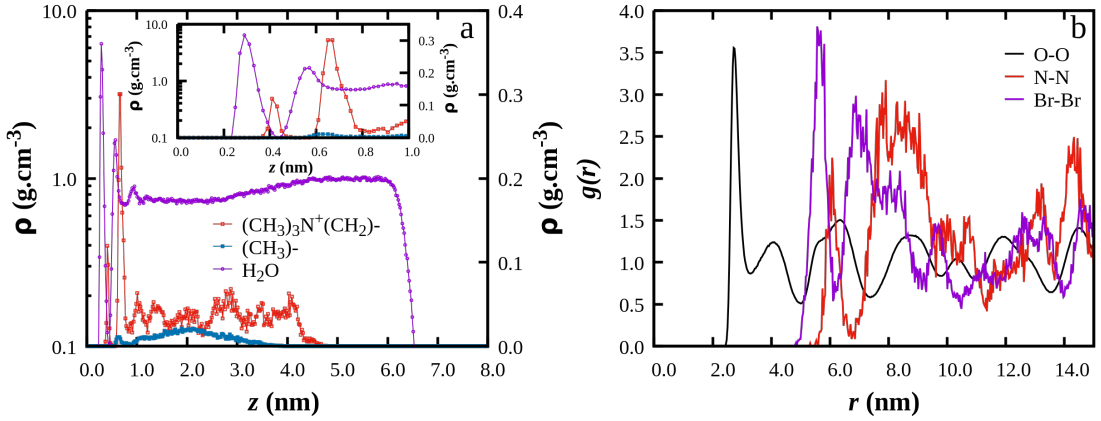

Figure 3.4: (a) Mass density of $(CH_3)_3N^+(CH_2)$–, $–CH_3$, and H_2O as a function of distance from the gold surface (b) In-plane pair correlations for water molecules, ammonium groups and bromide ions.

broader second peak in their RDFs, indicating that they are well-dispersed in this structured environment. Also, the RDF for bromide ions showed broader peaks compared to water and ammonium groups, indicating that bromide ions are more dispersed. This distribution suggests that the bromide ions are less tightly bound to specific layers and more evenly distributed within the micelle system.

In this study, we analyzed the energy landscape for a gold atom or nucleate approaching a gold (111) surface in a solution containing CTAB micelles. Figure 3.5 represents the Potential of Mean Force (PMF) profile derived from Steered Molecular Dynamics (SMD) simulations. Approximately 100 SMD simulations were conducted to map out the PMF, providing insights into the energy changes that gold atoms or nucleates experience as they navigate the solution environment and approach the surface. As a gold atom or nucleate moves toward the surface, it encounters an increase in energy upon reaching the periphery of a micelle. This is due to the strong interaction between the gold atoms and bromide ions. Bromide ions, along with their surrounding solvation shell, tend to accompany the gold atoms, forming partially negatively charged inter-micellar channels. These channels, located between closely spaced micelles, create zones with high bromide ion concentrations. In these regions, the electrostatic repulsion from the solvated bromide ions poses a barrier to the gold atom or nucleate, making it energetically challenging to progress toward the surface. The PMF profile in Figure 3.5 shows this energy barrier,

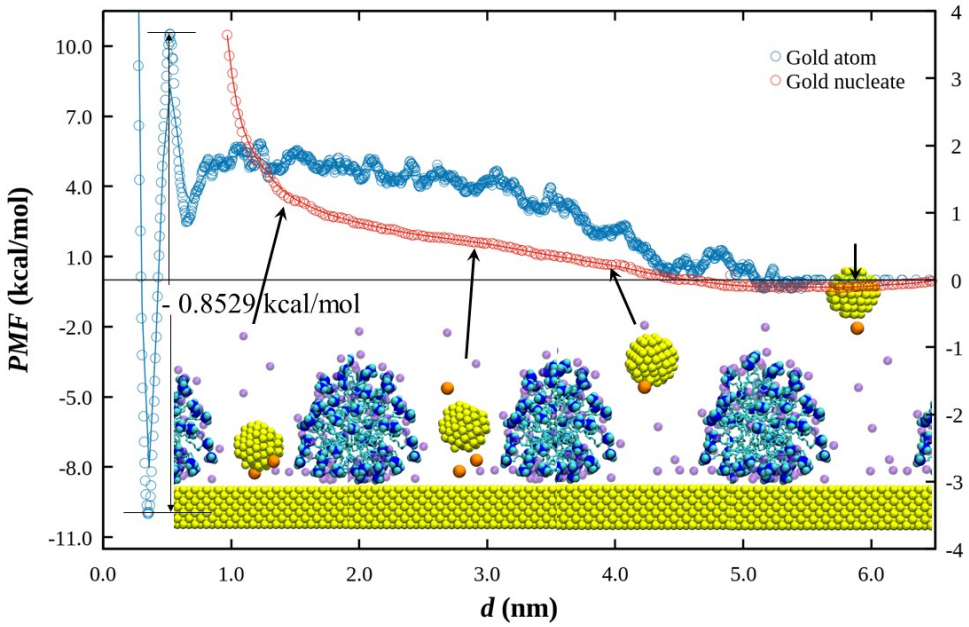

Figure 3.5: Potential of mean force with distance 'd', which is the distance between the centre of mass of the gold nucleate and the top of the surface. PMF profiles for a single gold atom on the left y-axis and that for gold nucleate on the right y-axis are represented as sky blue and red coloured circles, respectively. Snapshots at the bottom show the relative positions of nucleate and micelle while approaching the surface and accompany bromide ion(s) (orange sphere) accordingly marked at different distances from the surface. The black arrow indicates the position of nucleate as time progresses. Color codes are the same as in Figure 3.1, and water is not shown for clarity.

with the blue circles (left y-axis) representing the PMF for a single gold atom. As the gold atom approaches the inter-micellar region near the surface, the PMF reaches a high value of $\sim 9.14 \pm 0.3$ kcal/mol. This barrier prevents the gold atoms from directly reaching the surface and causes them to aggregate within the solution instead. Consequently, gold atoms tend to cluster, forming nucleates in the solution rather than individually nucleating on the surface. To further quantify the stability of gold nucleates in the solution, we calculated the PMF for a gold nucleate consisting of 137 atoms. The PMF for this nucleate is shown in red circles (right y-axis) in Figure 3.5, normalized to represent the energy per atom. When the gold nucleate is positioned above the interstitial zone between two micelles, the PMF is slightly negative, indicating an energetically favorable region for the nucleate. This is seen at around 3 nm from the surface, where the PMF reaches approximately -0.8529 kcal/mol, suggesting a stable configuration for the nucleate in this zone. As the nucleate progresses closer to the gold surface, it moves through areas with

increasingly higher bromide ion concentrations. These bromide ions begin to form pairs with the nucleate, as shown in the right-most snapshot in Figure 3.5, where bromide ions are visually clustered around the gold nucleate. Moving further into this interstitial zone, the gold nucleate-bromide complex experiences increased electrostatic repulsion from the surrounding bromide ions. This repulsion is reflected in the PMF profile, which becomes increasingly positive as the nucleate approaches the surface. The elevated bromide concentration and resulting electrostatic repulsion make the energy landscape steeper and less favorable, suggesting that the nucleate's journey through the micellar solution toward the surface is energetically costly. Interestingly, as the nucleate approaches the gold surface and enters this repulsive zone, the solvation shells of the bromide ions start to break down. At this point, the gold atoms within the nucleate can eventually deposit on the surface, releasing energy (-0.8529 kcal/mol). However, due to the high energy barrier, the nucleate remains more stable in the solution and is less likely to nucleate directly on the surface under these conditions. Instead, gold atoms tend to form aggregates within the micellar solution, stabilizing as nucleates. The challenging voyage of the nucleate through the inter-micellar zones highlights the role of the micellar environment and bromide ions in mediating the nucleation process. The energy barrier in these zones impedes the nucleate's direct access to the surface. This raises intriguing possibilities for studying the formation of gold nucleates through the aggregation of dispersed gold atoms in water and observing their structural evolution within the solution environment. To investigate the nucleation dynamics of gold atoms in a micelle-containing solution, a simulation was conducted with one hundred randomly distributed gold atoms. These atoms were tracked as they formed nucleates—clusters of gold atoms—within the micelle. Figures 3.6(a) and (b) showed how these gold nucleates of various sizes and shapes formed, eventually becoming encapsulated within the micelle rather than migrating towards the gold surface. In Figure 3.6(a), we observed the formation of gold nucleates within the micelle solution, with each cluster differing in shape and size. As these nucleates form, they approach the micelle's periphery and are gradually engulfed by it. Figure 3.6(b) further highlights this diversity in nucleate morphology, showing different shapes and sizes. The micelle structure is omitted for

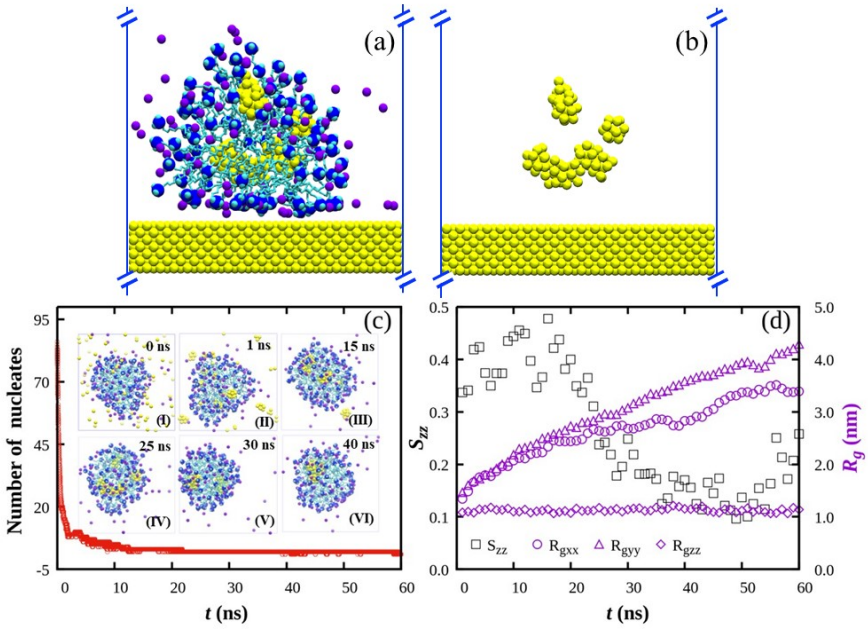

Figure 3.6: (a) Formation of Gold nucleates inside the micelle in solution. (b) Different shapes and sizes of the formed nucleates inside the micelle (micelle is not shown for clarity). (c) Formation of the number of nucleates as a function of time, Insets (I-VI) contain the snapshots of nucleate formation at 0, 1, 15, 25, 30, and 40 ns. (d) The change in order parameter (left axis) and radius of gyration (right axis) of micelle with time. Color codes are the same as in Figure 1; water is removed for clarity.

clarity in these snapshots, but we can infer that the micelle provides a stabilizing environment that prevents nucleates from diffusing towards the surface. Figure 3.6(c) depicted the evolution of the nucleates over the course of a 60 ns simulation, where the nucleate growth was closely monitored. At the start in Inset I, the individual gold atoms are well-dispersed in solution, each treated as a single nucleate. Within the first nanosecond, the nucleates begin to agglomerate rapidly, with the number of nucleates dropping sharply. By 1 ns, only 18 nucleates remained as smaller clusters merged as shown in Inset II. As the simulation progresses, the nucleates move toward the micelle's periphery. Here, we observed the micelle beginning to encapsulate the nucleates. At this stage, Inset III, the number of nucleates has reduced to around 9, with the largest consisting of 32 atoms and the smallest containing 3 atoms. Over time as shown in Inset IV-VI, nucleation dynamics slow down due to both steric hindrance within the micelle and reduced diffusion rates. The encapsulation by the micelle limits further growth and fusion of the nucleates. The gradual engulfing of these nucleates by the micelle results in them being held within the micelle

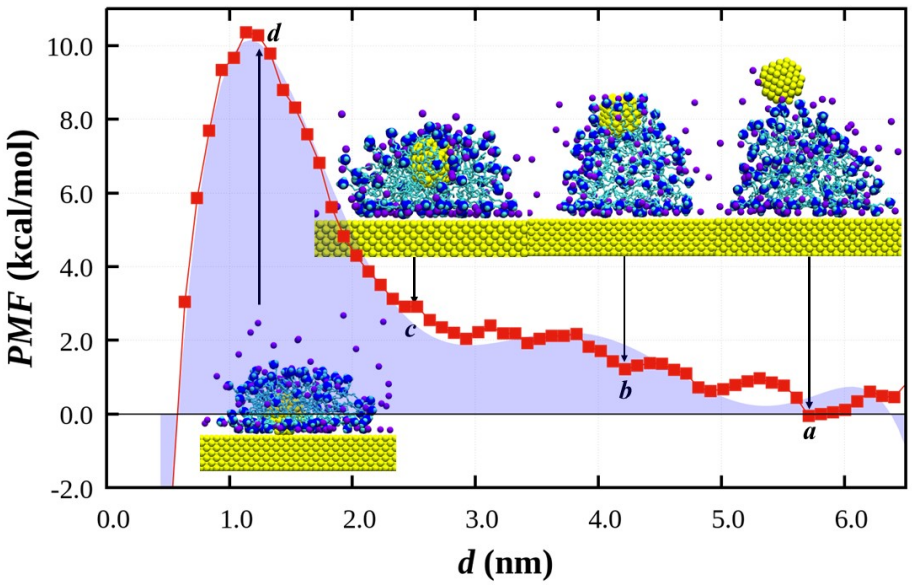

Figure 3.7: Potential of mean force with a distance between the centre of mass of gold nucleate and the top of the gold (111) surface.

structure rather than dispersing or reaching the surface. Figure 3.6d depicts the change in the micelle's structure during the formation of the nucleates. During the initial stages of rapid formation, the order parameter of the micelle rises, signifying a more bilayer-like structure inside the micelle. Gradually, a decline in the order parameter of the micelle is seen, signifying an introduction of randomness into the system. Upon the incorporation of nucleates inside the micelle, the micelle undergoes deformation to accommodate them. The gradual engulfment and consequent rearrangement of molecules move the nucleates towards the centre, enabling it to achieve its target ordering of ~ 0.3. The different components of the radius of gyration indicate that the shape remains unchanged perpendicular to the surface, while it expands in the xy plane. However, the nucleates did not reach the gold surface. It hints at the existence of a high energy barrier, and quantification will help us understand their evolution process.

To understand the energy landscape of a gold nucleate engulfed within a CTAB micelle and its subsequent transition toward a gold (111) surface, we calculated the potential of mean force (PMF) using Umbrella Sampling. Figure 3.7 presents the PMF profile for this system, with energy values shifted to set the most stable state as the reference (ground state) energy. The PMF analysis reveals critical nucleate interaction stages with the mi-

celle and the surface. Initially, when the gold nucleate is in close proximity to the micelle, strong interactions with bromide ions facilitate its rapid attachment to the micelle. This forms a highly stable state, marked as "a" in Figure 3.7, representing the lowest energy state of the system. Following this, the favorable interaction of the nucleate with the gold atoms drives the micelle to engulf it. However, this process requires the micelle to undergo molecular rearrangement, necessitating energy input to accommodate the nucleate within its structure. This reorganization introduces an energy barrier of 1.21 kcal/mol (point "b" in Figure 3.7). Overcoming this barrier allows the micelle to encapsulate the nucleate fully. Once the energy barrier is surpassed, the micelle spontaneously engulfs the nucleate, as indicated by a sharp drop in the PMF (point "c"). This encapsulation stabilizes the nucleate due to enhanced configurational entropy in the micelle's hydrocarbon chains, forming a well-organized and stable complex. However, for the nucleate to be released from the micelle onto the gold surface, the system must climb a steep energy barrier of 10.36 ± 0.3 kcal/mol as indicated by point "d" in Figure 3.7. This significant barrier is primarily due to the strong stabilization and structural layering of the micelle on the gold surface, mediated by water molecules. Breaking this layering and releasing the nucleate requires substantial energy input, such as heat or work. The feasibility of alternative approaches to overcome this energy barrier is discussed further by analyzing structural evolution.

Figures 3.8a and b provide a detailed visualization of the micelle's deformation upon encapsulating the nucleate and during its transition toward the gold surface. Figure 3.8a (top view) shows how the micelle deviates from its spherical shape as the nucleate is pushed closer to the surface. In Figure 3.8b (side view), the deformation is observed to occur on both sides of the micelle, confirming its structural flexibility during the process. These deformations highlight the micelle's ability to adapt dynamically to encapsulate and transport the nucleate while resisting direct release onto the surface. We analyzed the structural evolution of the CTAB micelle as the nucleate moves closer to the gold surface by calculating the order parameter and the radius of gyration (R_g) of the micelle at different positions of the nucleate. Figure 3.8c depicts these changes, providing insights into the

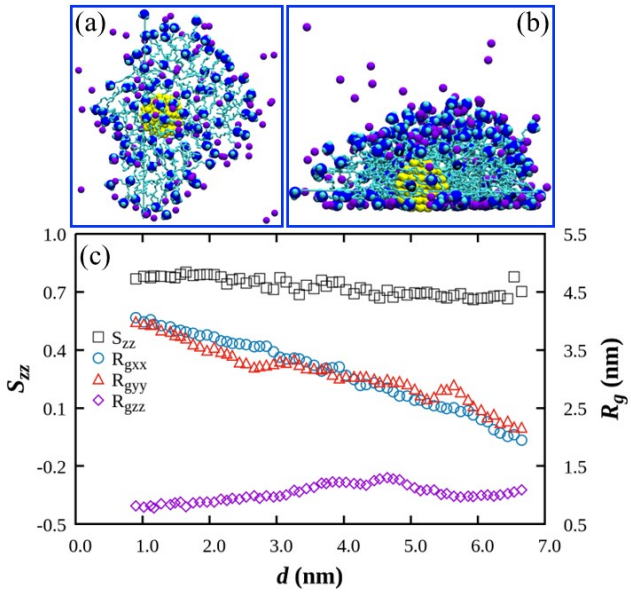

Figure 3.8: (a) Top view, (b) Side view, (c) Order parameter and variation of Radius of gyration with the distance between the center of mass of nucleate and gold (111) surface.

micelle's structural behavior during this process.The order parameter increases as the nucleate approaches the surface, indicating greater molecular ordering within the micelle. This higher degree of ordering reflects a transition towards a more organized structure, likely in response to the nucleate's influence. The radius of gyration was also examined to understand the size and overall shape of the micelle during the nucleate's progression. Figure 3.8c shows the variation in the components of R_g, ($R_{g_{xx}}$, $R_{g_{yy}}$, and $R_{g_{zz}}$) with the distance between the nucleate's center of mass and the gold surface. As the nucleate traverses through the micelle, the micelle elongates in the x and y directions, as indicated by the gradual increase in R_{gxx} and R_{gyy}. Concurrently, a decrease in R_{gzz} suggests that the micelle's shape transitions towards a bilayer-like configuration.[156] This deformation is corroborated by the increasing trend in the orientation order parameter, which further confirms the shift towards a bilayer-like structure. The increased molecular ordering and structural adaptation emphasize the micelle's dynamic ability to respond to external stimuli, such as the presence of the nucleate, ultimately leading to the observed changes in its morphology and configuration.

3.4 Summary

In summary, this work has yielded insights into the voyage of gold nucleates to the gold surface for the growth of the surface. We conducted a comprehensive molecular dynamics simulation-based investigation to gain a deeper understanding of this growth process. This investigation allowed us to construct a detailed free energy landscape, enabling us to decipher the intricate mechanism governing the growth of nanocrystals on the gold (111) surface in the presence of CTAB surfactant. Notably, our findings indicate the presence of a formidable energy barrier associated with this process. Even larger nucleates encounter similarly steep energy barriers. Nucleates find a pathway into the spherical micelles' core, potentially allowing their growth to continue. This intriguing revelation opens the door to manipulating and directing nanocrystal growth through external means that elongate or distort the shape of the micelles. In sum, our study enhances our understanding of micellar structures and their impact on nanocrystal growth and hints at future research directions. The manipulation of micellar structures to control nanocrystal growth represents an exciting avenue for further exploration in nanomaterial synthesis. These findings contribute to the broader knowledge surrounding nanoscience and materials chemistry, offering new perspectives and opportunities for innovation in nanotechnology.